3-D modelling of the magnetic fields due to ocean tidal flow

Alexei Kuvshinov and Nils Olsen

Danish Space Research Institute/Center for Planetary Science, Juliane Maries Vej 30, DK-2100 Copenhagen, Denmark, e-mails: alexei@dsri.dk; nio@dsri.dk)

Summary. Recently Tyler et al. (2003) demonstrated that the magnetic fields generated by the lunar semidiurnal (M_2) ocean flow can be clearly identified in magnetic satellite observations. They compared their numerical simulations of magnetic fields due to the M_2 tide with CHAMP observations and found close agreement between observations and predictions. Their three-dimensional (3-D) conductivity model consists of a surface thin shell of variable conductance and an insulating mantle underneath. Some discrepancies between observations and predictions have been addressed to the absence of a coupling between the surface shell and the mantle. Here we performed model studies of the magnetic signals due to ocean tidal flow in order to answer the following questions. (1) How does the inclusion of a conducting mantle affect the magnetic signals of the M_2 tide at CHAMP altitude? (2) Are magnetic signals from other tidal components detectable at CHAMP altitude? (3) What amplitude has the magnetic M_2 tide at Ørsted altitude? The 3-D conductivity model that we consider incorporates a thin shell and either a radially symmetric or a 3-D mantle underneath. Our model studies demonstrate that including a conducting mantle yields significant changes of the magnetic M_2 oceanic signals, with peak-to-peak values at CHAMP altitude of order 3 nT. The magnetic signals due to other prominent ocean tidal modes (like K_1 and O_1) are below 0.5 nT at CHAMP altitude. The M_2 peak-to-peak magnetic signal at Ørsted altitude is of order 1 nT.

Key words: ocean tides, magnetic fields variation, electromagnetic induction, three-dimensional modellings

1 Modelling approach

To calculate the magnetic fields due to global ocean tides we used the numerical solution of Kuvshinov et al. (2002a), but with the modifications introduced by Avdeev et al. (2002). The solution is based on a volume integral equation (IE) approach and allows simulating the electromagnetic (EM) fields, excited by arbitrary sources in three-dimensional (3D) spherical models of electric conductivity. These 3-D models consist of a number of anomalies of conductivity $\sigma_{3D}(\vartheta,\varphi,r)$, embedded in a host section of conductivity $\sigma_b(r)$. Here ϑ,φ and r are co-latitude, longitude and the distance from the Earth's centre, respectively. Maxwell's equations in the frequency domain,

$$\nabla\times\mathbf{H}=\sigma\mathbf{E}+\mathbf{j}^{\text{ext}}\ , \tag{1}$$

$$\nabla\times\mathbf{E}=i\omega\mu_{\text{o}}\mathbf{H}\ , \tag{2}$$

are reduced, in accordance with the modified iterative-dissipative method (Singer, 1995), to a scattering equation of specific type (cf. Pankratov et al., 1997)

$$\boldsymbol{\chi}(\mathbf{r})-\int\limits_{V^{mod}}K(\mathbf{r},\mathbf{r}')R(\mathbf{r}')\boldsymbol{\chi}(\mathbf{r}')dv'=\boldsymbol{\chi}_{\text{o}}(\mathbf{r})\ , \tag{3}$$

which is solved by the generalized bi-conjugate gradient method (Zhang, 1997). In eqs. (1)-(3) $\mathbf{j}^{\text{ext}}$ is the exciting current density, the time-harmonic dependency is $e^{-i\omega t}$, μ_{o} is the magnetic permeability of free space, $i=\sqrt{-1}$, $\omega=2\pi/T$ is the angular frequency, T is the period of variations, $\sigma(\mathbf{r})$ is the model conductivity distribution, $\mathbf{r}=(\vartheta,\varphi,r)$, $\mathbf{r}'=(\vartheta',\varphi',r')$, V^{mod} is the modelling region and

$$R = \frac{\sigma - \sigma_o}{\sigma + \sigma_o}, \tag{4}$$

$$K(\mathbf{r},\mathbf{r}') = \delta(\mathbf{r}-\mathbf{r}')I + 2\sqrt{\sigma_o(r)}G_o^e(\mathbf{r},\mathbf{r}')\sqrt{\sigma_o(r')}\,, \tag{5}$$

$$\boldsymbol{\chi}_o = \int_{V^{mod}} K(\mathbf{r},\mathbf{r}')\frac{\sqrt{\sigma_o(r')}}{\sigma(\mathbf{r}')+\sigma_o(r')}\mathbf{j}^s(\mathbf{r}')dv', \tag{6}$$

$$\boldsymbol{\chi} = \frac{1}{2\sqrt{\sigma_o}}((\sigma+\sigma_o)\mathbf{E}^s + \mathbf{j}^s)\,, \tag{7}$$

$$\mathbf{j}^s = (\sigma-\sigma_o)\mathbf{E}^o\,, \tag{8}$$

$$\mathbf{E}^o = \int_{V^{ext}} G_o^e(\mathbf{r},\mathbf{r}')\mathbf{j}^{ext}(\mathbf{r}')dv'\,, \tag{9}$$

where $\delta(\mathbf{r}-\mathbf{r}')$ is Dirac's delta function, I is the identity operator, V^{ext} is the volume occupied by exciting current $\mathbf{j}^{ext}$, $\mathbf{E}^s = \mathbf{E} - \mathbf{E}^o$ is the scattered electric field, G_o^e is the 3×3 Green's tensor of the 1-D reference conductivity $\sigma_o(r)$. Note that, in order to provide optimum efficiency of scattering equation solution, $\sigma_o(r)$ is chosen in a special way (cf. Singer, 1995;) and generally differs from $\sigma_b(r)$ at depths where the anomalies are located.

Once $\boldsymbol{\chi}$ is determined from the solution of (3), the scattered electric field, $\mathbf{E}^s$, is obtained from (7) and the magnetic field, $\mathbf{H}$, at the observation points, $\mathbf{r} \in V^{obs}$, is calculated as

$$\mathbf{H} = \int_{V^{ext}} G_o^h(\mathbf{r},\mathbf{r}')\mathbf{j}^{ext}(\mathbf{r}')dv' + \int_{V^{mod}} G_o^h(\mathbf{r},\mathbf{r}')\mathbf{j}^q(\mathbf{r}')dv'\,, \tag{10}$$

with

$$\mathbf{j}^q = (\sigma-\sigma_o)(\mathbf{E}^o + \mathbf{E}^s)\,. \tag{11}$$

The explicit expressions to calculate the elements of Green's tensors G_o^e and G_o^h are presented in Appendix of Kuvshinov et al. (2002a). For our problem the exciting current density, $\mathbf{j}^{ext}$, is calculated as

$$\mathbf{j}^{ext} = \sigma_w(\mathbf{V}\times\mathbf{B}^m)\,, \tag{12}$$

where "×" denotes the vector product, σ_w = 3.2 S/m is the sea water conductivity, $\mathbf{V}$ is the water transport (depth integrated velocity) due to ocean tides, taken from the TPXO6.1 global tidal model of Egbert & Erofeeva (2002), and $\mathbf{B}^m$ is the main magnetic field taken from IGRF 2000.

2 Comparison of two solutions

To check our integral equation (IE) solution we compare it against the finite difference (FD) solution of Tyler et al. (2003). In both cases the conductivity model consists of a surface thin shell and an insulating mantle underneath. A realistic distribution of the shell conductance is obtained by considering contributions from sea water and from sediments as described in Kuvshinov et al. (2002b). Fig. 1 presents the vertical component of the magnetic field, B_r, due to the M_2 tide (period = 12.42 hours) at ground, as given by Tyler et al. (2003) (upper

panel) and by IE method (lower panel). Tyler's results are for a mesh of 2°×2° resolution, while our results are for a mesh of 1°×1° resolution. The good agreement between the two results verifies both approaches.

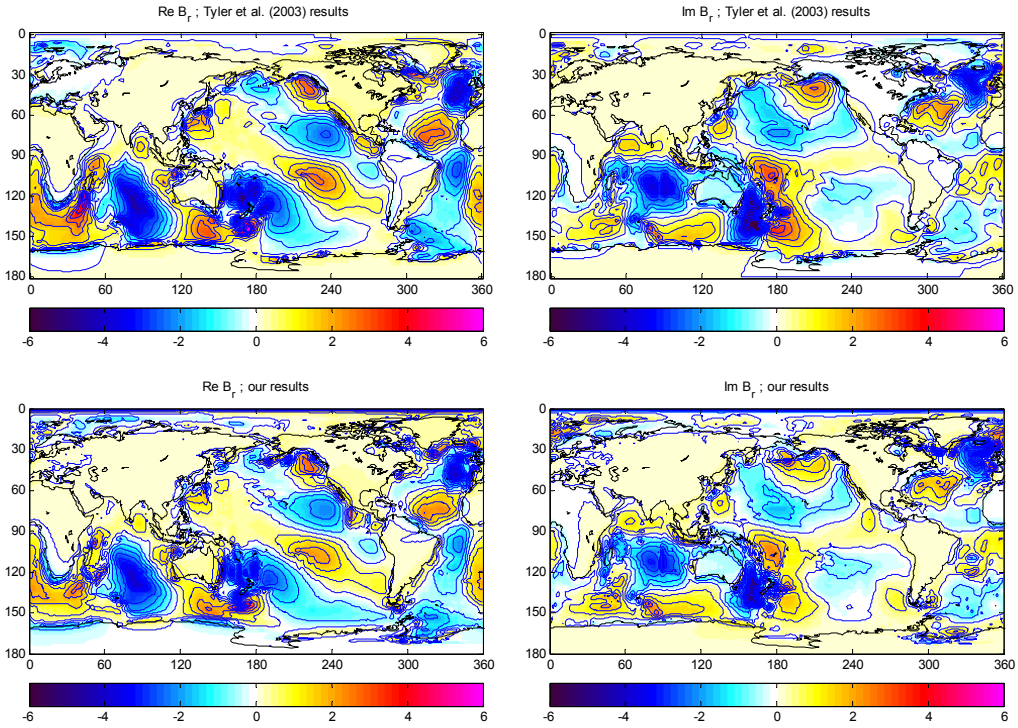

Fig. 1. B_r (nT) at the ground from M_2 tide obtained by Tyler et al. (2003) (upper panels) and with our IE solution (lower panels). The results are for an insulating mantle.

3 Simulations with conducting mantle

In order to investigate how the inclusion of a conducting mantle affects the magnetic signal of the M_2-tide at CHAMP altitude we performed simulations using a conductivity model that consists of a laterally inhomogeneous surface shell (same as in previous section) and a 1-D mantle section underneath. Fig. 2 presents the M_2 tide scalar anomalies *dF* at CHAMP altitude (430 km); model resolution is 1°×1°. The upper panels show the results obtained for an insulating mantle, whereas the lower ones show those for a 1-D conducting mantle which is based on the 3-layer model of Schmucker (1985), but with a 100 km lithosphere of 3000 Ωm. Comparing the results it is seen that in general the pattern remains the same, but the magnitude of the signals decreases when a conducting mantle is incorporated in the model.

Next were carried out simulations for two other prominent tidal components. Fig. 3 shows the scalar anomalies *dF* at CHAMP altitude due to the diurnal tides K_1 (period = 23.9 hours; upper panel) and O_1 (period = 25.8 hours; lower panel) for a conducting mantle. One can see that the magnetic signals due to these tides are below 0.5 nT at CHAMP altitude.

Finally we calculated the M_2 tide scalar anomalies *dF* at Ørsted altitude (800 km) for the same conductivity model. As it is expected (see Fig. 4) the magnitude of the signal is decreased and becomes smoother compared with that at CHAMP altitude.

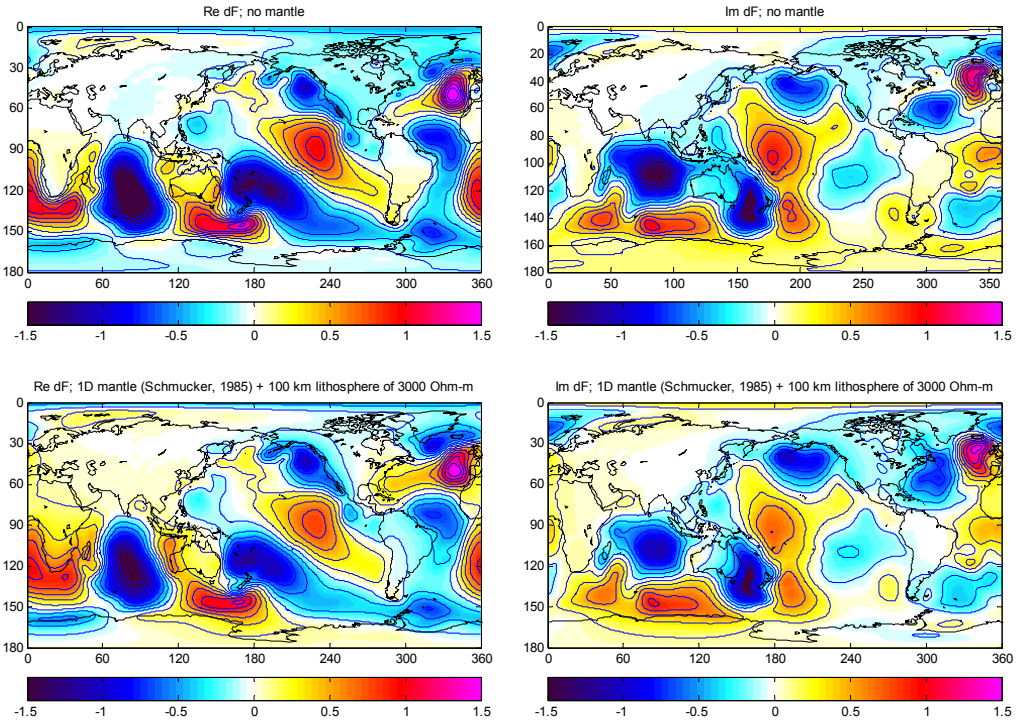

Fig. 2. M_2 tide scalar magnetic field dF (nT) at $h = 430$ km altitude for the models with insulating (upper panels) and conducting (lower panels) mantle, respectively.

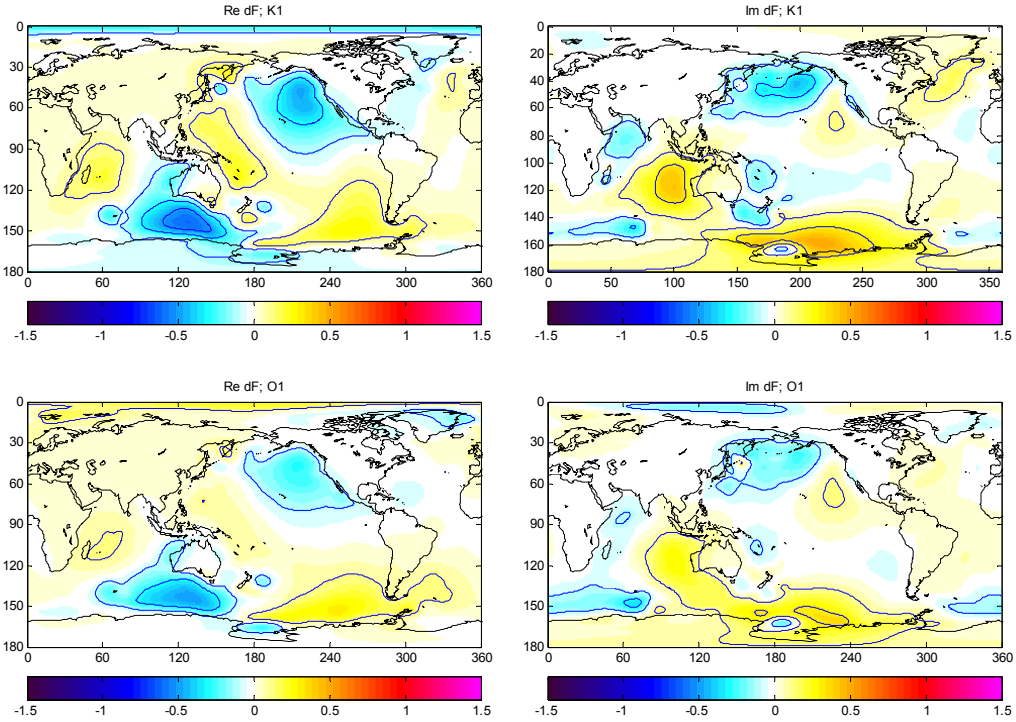

Fig. 3. Scalar anomaly dF (nT) at $h = 430$ km altitude due to the K_1 (upper panels) and O_1 (lower panels) tidal modes.

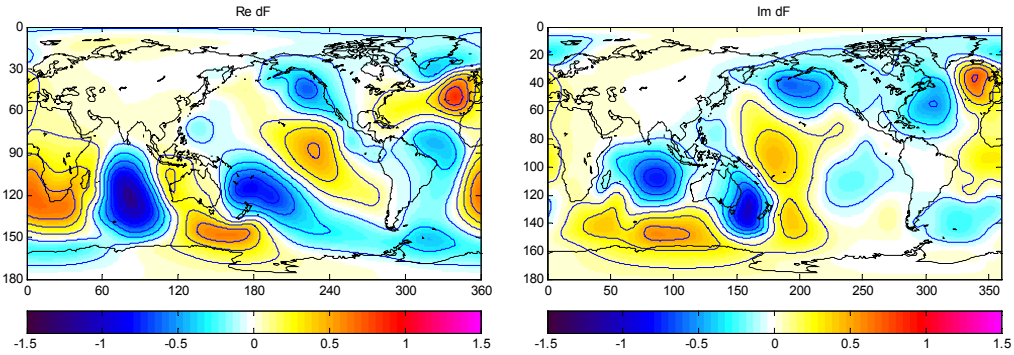

Fig. 4. M_2 tide scalar magnetic field dF (nT) at $h = 800$ km altitude.

4 Comparison with CHAMP observations

Fig. 5 shows the amplitudes of high-pass filtered modelled magnetic M_2 scalar anomaly, averaged over all latitudes between –60° and +60°, in dependence on longitude. These results are for different mantle conductivity models beneath the surface shell. For the "nonuniform lithosphere" model, the resistivity of the uppermost 100 km is set to 300 Ωm beneath the oceans, whereas that beneath the continents is set to 3000 Ωm. The largest difference in the magnetic field at CHAMP altitude is found when comparing the results for an insulating with that of a realistic (conducting) mantle. Also shown are the CHAMP results by Tyler et al. (2003). Note that they have been derived using a slightly different filtering approach.

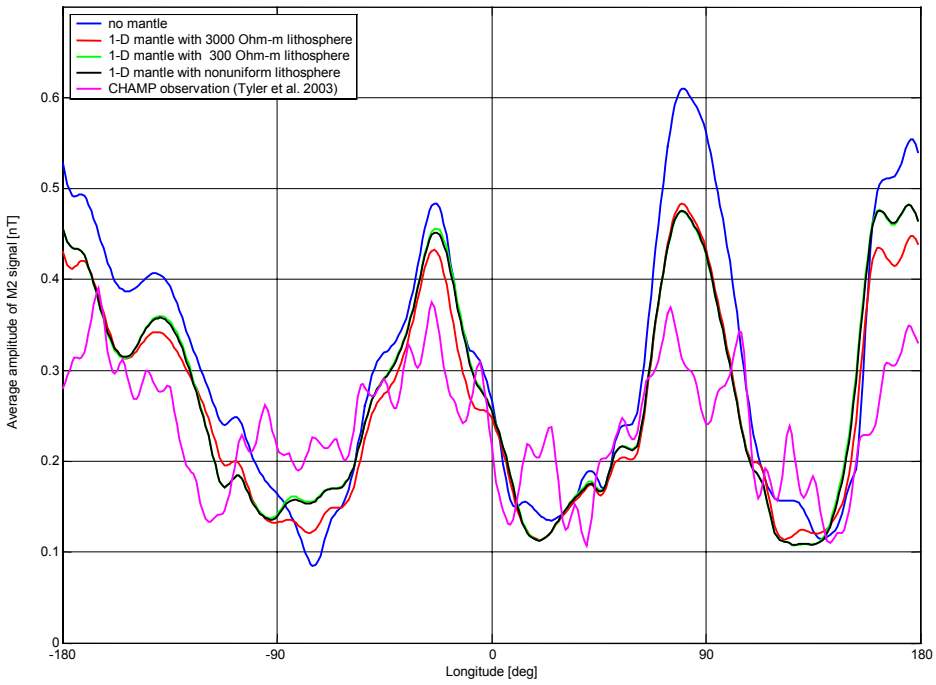

Fig. 5. Meridionally averaged magnetic signal amplitudes (nT) at CHAMP altitude, calculated for various mantle conductivity models. Also shown are observational results, obtained from CHAMP scalar data by Tyler et al. (2003).

5 Conclusions

We presented the results of 3-D simulations of the magnetic field variations caused by global ocean tidal flow. Our model studies demonstrate that considering a conducting mantle yields significant changes of the M_2 magnetic signals, with peak-to-peak values at CHAMP altitude of order 3 nT. The magnetic signals due to other prominent ocean tidal modes (like K_1 and O_1) are below 0.5 nT at CHAMP altitude. The M_2 peak-to-peak magnetic signal at Ørsted altitude is of order 1 nT.

Aknowledgements

We would like to thank Stefan Maus and Rob Tyler for providing us with data for the study comparisons.

References

Avdeev D, Kuvshinov A, Pankratov O, Newman G (2002) Three-dimensional induction logging problems, Part I: An integral equation solution and model comparisons. Geophysics 67: 413-426.

Egbert G, Erofeeva S (2002) Efficient inverse modeling of barotropic ocean tides. J of Oceanic and Atmosph. Technol. 19:183-204

Kuvshinov A, Avdeev D, Pankratov O, Golyshev S, Olsen N (2002a) Modelling electromagnetic fields in 3D spherical Earth using fast integral equation approach. 3D Electromagnetics, Chapter 3: 43-45, Elsevier.

Kuvshinov A, Olsen N, Avdeev D, Pankratov O (2002b) Electromagnetic induction in the oceans and the anomalous behaviour of coastal C-responses for periods up to 20 days. Geophys Res Lett 29: 2001GL014409.

Pankratov O, Kuvshinov A, Avdeev D (1997) High-performance three-dimensional electromagnetic modeling using modified Neumann series. Anisotropic case. J Geomagn. Geoelectr 49:1541-1547.

Schmucker U (1985) Magnetic and electric fields due to electromagnetic induction by external sources, electrical properties of the earth interior. Landolt-Boernstein New Series Group, 5/2b, Springer Verlag, Berlin.

Singer B (1995) Method for solution of Maxwell's equations in non-uniform media. Geophys J Int 120:590-598.

Tyler RH, Maus S, Luhr H (2003) Satellite observations of magnetic field due to ocean tidal flow. Science 299:239-241.

Zhang S-L (1997) GPBi-CG: generalized product-type methods based on Bi-CG for solving non symmetric linear systems. SIAM J Sci Comput 18: 537-551.